ASIAN JOURNAL OF PHARMACEUTICAL AND CLINICAL RESEARCH

INNOVARE ACADEMIC SCIENCES
Knowledge to Innovation

Vol 9, Issue 4, 2016

Online - 2455-3891
Print - 0974-2441

Research Article

EXPLORING DEFLUORIDATION CAPACITY OF TURMERIC ON INDUSTRIAL SEWAGE

TEJ PRATAP SINGH[1], APOORVA TRIPATHI[2], DEEPANKAR DEV PANDEY[2], MAJUMDER CB[1]*

[1]Department of Chemical Engineering, IIT Roorkee, Roorkee - 247 667, Uttarakhand, India. [2]Department of Chemical Engineering, BIET Jhansi, Jhansi - 284 128, Uttar Pradesh, India. Email: cbmajumder@gmail.com

Received: 06 April 2016, Revised and Accepted: 15 April 2016

ABSTRACT

Objective: This research was carried out for developing a low-cost agro-based biosorbent for defluoridation of wastewater. Here, we investigated the defluoridation capacities of simple turmeric and MnO_2-coated turmeric.

Methods: The defluoridation capacity of turmeric had been investigated through batch sorption techniques. In the batch sorption technique, the effect of various parameters such as adsorbent dose, initial fluoride concentration, and pH had been studied, and these parameters are optimized for maximum fluoride removal efficiency. Each adsorbent was characterized using various techniques such as Fourier transform infrared spectroscopy, scanning electron micrograph, and Energy Dispersive Analysis of1 X-Ray. The adsorption kinetics had been studied through different kinetics models such as intra-particle diffusion model and pseudo-first order model. For adsorption equilibrium, we studied the conventional equilibrium models such as Langmuir isotherm model and Freundlich isotherm model.

Results: The result of the performed experiments shows that for turmeric and MnO_2-coated turmeric, the values of pH, adsorbent dose, initial concentration, and contact time were 7 and 6, 12 and 14 g/l, 20 and 20 mg/l, 60 and 75 minutes at which optimum defluoridation of about 89.9% and 94.34% occurs, respectively.

Conclusion: The result obtained from the experiments shows that the MnO_2 coating has increased the defluoridation capacity of the turmeric.

Keywords: Defluoridation, Turmeric, MnO_2-coated turmeric, Fourier transform infrared spectroscopy, Scanning electron micrograph, Energy Dispersive Analysis of X-Ray, Langmuir isotherm, Freundlich isotherm.

INTRODUCTION

Fluoride is an inorganic compound whose small quantity is necessary for human beings, but its large consumption is very harmful. The WHO has specified that the fluoride in the drinking water should lie in the range of 0.5-1.0 mg/l. If this concentration exceeds in the human body, it leads to various diseases commonly dental and skeletal fluorosis, and if the fluoride accumulation is very large, it changes the DNA structure [1,2]. Fluoride contamination is an increasing global concern as an excess of which can cause the toxic effects on many biological systems [3-6]. Around 25 countries throughout the world are facing consequences of fluoride contamination. In India, about 19 states were severely affected from fluoride contamination in drinking water [7] and more than 6 million children suffer from skeletal, non-skeletal, or dental fluorosis [5,8]. Thus, due to scarce resources of drinking water, it is necessary to treat the fluoride contaminated water before its consumption for which different defluoridation techniques were used such as adsorption [9,10], chemical treatment [11,12], ion-exchange [13], membrane separation, electrolytic defluoridation, and electro dialysis. In recent years, various attempts were made for developing a more cost-effective F^- sorbents such as silica gel [14], spent catalyst [15], fly ash [16], zeolites [17], and bone char [18]. Among all the existing techniques, adsorption is more cost effective and simple. Thus, in this study, the fluoride adsorption potential of MnO_2-coated turmeric and turmeric has been studied through batch wise biosorption, and the comparison has been done for finding the best adsorbent between the two.

METHODS

Preparation of biosorbents

A low-cost biosorbent, turmeric is obtained from the local market of Roorkee, Uttarakhand, India. All the required chemicals were of analytical grade and obtained from E. Merck India Limited, Mumbai, India. Initially, the turmeric was washed with tap water after which it is treated with 0.1 N HCl and 0.1 N NaOH in the same order. Then, the turmeric was washed thoroughly using distilled water and dried by exposing it to sunlight for 2-3 days and then in an oven at 80°C for 24 hrs as shown in Fig. 1: (a and b) Turmeric after washing. After drying, the turmeric was crushed and sieved to obtain particle size of 475 µm and then coated by MnO_2 for better adsorption studies.

For preparing the MnO_2-coated turmeric, we took a sample of 27 g of $KMnO_4$ in a beaker with 21 ml of distilled water which is kept in water bath for 15 minutes at a temperature of 90°C. Now, 2 g of turmeric was added in the solution and suspension was given a 10 minutes water bath to settle the suspension. This is followed by addition of 300 ml of 2 M HCl, which is preceded by water bath heating for 30 minutes. After the completion of the reaction, the solid was cooled and washed with distilled water and 0.05 M perchloric acid until the run-off water was clear.

Adsorption experiments

To prepare 100 mg/l fluoride stock solution, 0.221 g of anhydrous sodium fluoride (NaF) was dissolved in 1 l of millipore water. This solution is used to prepare test solution with fluoride concentration of 20 mg/l which is common value of sewage water fluoride concentration. Experiments were carried out in 250 ml conical flasks, with 50 ml test solution at (29±1)°C in a conical flask in horizontal incubator shaker. At the end of desired contact time, the conical flask was removed from the shaker. Subsequently, samples were filtered using Whatman No. 42 filter paper, and filtrate was analyzed for residual fluoride concentration by SPADNS method, described in the standard method of examination of wastewater and water [19]. Batch study was conducted for determining the optimum conditions for fluoride removal, in which the effect of pH, adsorbent dose, contact time, and initial fluoride concentration in adsorption was studied. pH was adjusted using 0.1 N HCl or 0.1 N NaOH on fixed quantity of adsorbent.

Spectrophotometric methods

In this technique, compound of a metal such as aluminum, iron, thorium, zirconium, lanthanum, or cerium reacts with an indicator dye to build a complex of small dissociation constant. This complex reacts with fluoride to give a new complex. Because of the transformation in the configuration of the complex, the surface assimilation spectrum also shifts relative to the spectrum for the fluoride-free reagent solutions. This alteration can be observed using a spectrophotometer. One of the essential dyes employed is trisodium 2-(parasulfophenylazo)-1, 8-dihydroxy-3, and 6-naphthalene disulfonate, generally recognized as SPADNS. Erichrome Cyanine R is one more usually used dye. The dye reacts with metal ions to give a colored complex. In the SPADNS method, zirconium reacts with SPADNS to build a red complex. Fluoride discolors the red of the complex, and therefore, the alteration in absorbance can be calculated using the spectrophotometer.

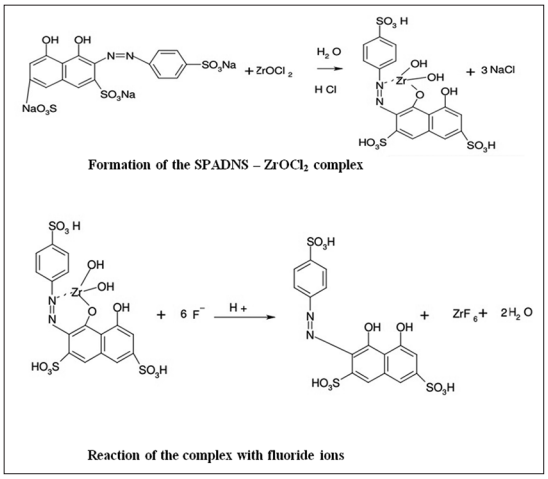

Recipe for SPADNS solution

$$\frac{\text{Mg of fluoride}}{\text{Litre}} = \frac{A}{\text{Sample(mL)}} \times \frac{B}{C}$$

Where,

A represents fluoride obtained by curve (mg)

B represents diluted sample final volume (ml)

C represents diluted sample volume worn for the development of color.

$$\frac{\text{Mg of fluoride}}{\text{Litre}} = \frac{A_0 - A_x}{A_0 - A_1}$$

Where,

A_0 represents absorbance at zero fluoride concentration

A_1 represents absorbance at fluoride concentration of 1 mg/l

A_x represents absorbance of the sample prepared.

RESULT AND DISCUSSION

Effect of pH

The relationship between pH scale and removal of fluoride was studied within the domain of 2-12 and obtained results are shown in Fig. 2.

The role of pH becomes vital in the process of adsorption on bio-adsorbents. As illustrated in Fig. 2, it is concluded that the removal efficiency of the adsorbents is related to the pH of the sample. The results obtained confirm a strong relationship among adsorption on bio-

Fig. 1: (a and b) Turmeric after washing AQ3

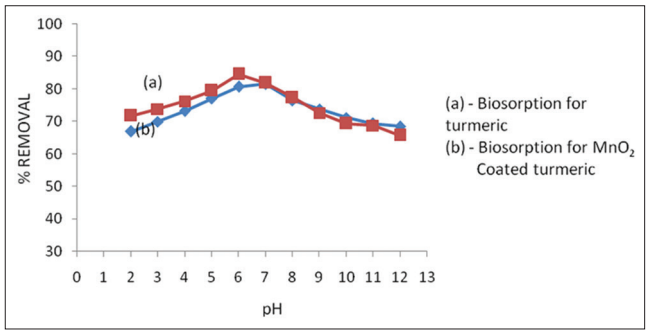

Fig. 2: The effect of pH on fluoride removal

adsorbent and pH of the sample. It is noted that with increase in pH in the range of 1-7 results in more adsorption of fluoride on bio-adsorbent. When maximum adsorption was observed, pH of the solution was 6.0 and 7.1 for MnO_2-coated turmeric and turmeric, respectively, at the end of 1.15 hrs. Many researchers in their report focused on the point that biosorption process is more comfortable in aqueous phase pH and the functional groups on the biosorbent, and their ionic states (at particular pH) [20-22]. Micro-molecules have groups such as carboxyl, alcohol, phosphate, thiol, phenol, and amino in most of biosorption process. The process reaches forward when protonation and deprotonation of functional groups happen on the surface of bio-adsorbent [23]. The ionic form of fluoride in the solution and the electric charge on the bio-adsorbent is governed by pH of solution where it is shown that overall charge on the surface of bio-adsorbent is non-negative. Positive charge is present on the surface of bio-adsorbent form bonds with negatively charged fluoride ions. In the case of turmeric, no effect of pH was seen as it shows maximum adsorption at neutral pH (pH=7). This means the surface turmeric is the cationic type (H^+) in nature [24]. When the value of pH is lower (<7), the surface of the adsorbent gets positively charged and occurred, probably anionic exchange sorption. In acidic medium because of the protonation, action on the surface functional groups such thiol, amino carboxyl, etc., exerts positive charge on the surface. Relative sorption inhibition that occurred at basic pH (>7) range might be assigned to the increase of hydroxyl ion leading to the formation of aqua-complexes; thereby, desorption occurred [25].

According to the various study of optimization of pH adsorption on bio-adsorbent is mostly noted in the acidic range of the pH (<7). In the present case, we noted that fluoride removal is observed in less acidic range thus making it beneficial and economy wise a good model for removal of halide from waste water. To understand the fluoride sorption behavior under different pH values, the following reactions are considered [26,27]:

$$HF \leftrightarrow H^+ + F^-$$

$$=SOH + H^+ \leftrightarrow =SOH_2^+$$

$$=SOH + OH^- \leftrightarrow =SO^- + H_2O$$

$$=SOH_2^+ + F^- \leftrightarrow =SF + H_2O$$

$$=SOH + F^- \leftrightarrow =SF + OH^-$$

Where =SOH, =SOH_2^+, and =SO^- represent the neutral, protonated, and deprotonated sites on turmeric and MnO_2-coated turmeric, and =SF is the active site-fluoride complex (S=turmeric/MnO_2-coated turmeric).

Dose optimization

Removal efficiency of fluoride is strongly related to the concentration of adsorbent dose in the test sample. With increasing dose of adsorbent in the sample removal of fluoride increases as shown in Fig. 3.

In starting, removal of fluoride increases with the increase in dose up to an extent after which very slight change is noted in the removal of fluoride meaning the curve becomes flat indicating no change in fluoride removal even with increasing dose. Adsorbents do have surface and pore volumes due to which adsorption increases initially with increase in dose, but when pore volume and surface reaches saturation, there is very little effect of increasing dose. Removal efficiency for MnO_2-coated turmeric and turmeric increases from 70.23% to 80.952% and 62.79% to 76.59%, respectively, when the dose varies from 2 to 20 g/l. However, there is no major change in removal efficiency for fluoride when dose is varied from 12 to 20 g/l and 14-20 g/l for turmeric and MnO_2-coated turmeric, respectively. This happens due to overlapping of active sites at a higher dosage, which reduces net surface area [23].

Effect of contact time

It is observed that the exclusion of fluoride ions increases with increase in contact time to some level at optimum pH and dose. Further increase in contact time does not increase the uptake due to deposition of fluoride ions on the available adsorption pore volume and surface area on bio-adsorbent materials as shown in Fig. 4.

Fig. 4 explains the efficiency of removal of fluoride by two considered bio-adsorbents (turmeric and MnO_2-coated turmeric) at different contact times. However, it came near to an almost constant value, denoting achievement of equilibrium. In the current case, the equilibrium times were recorded as 60 and 75 minutes for MnO_2-coated turmeric and turmeric, respectively. The initial peak portion revealed the high sorption uptake of the fluoride ions onto adsorbents. The second stage assigns the sluggish uptake of fluoride ions that showed the usage of all active sites over the adsorbents surface and fulfillment of saturation or equilibrium stage. The third stage indicated the saturation stage in which, the sorption uptake was comparatively less [28].

Effect of initial fluoride concentration

The outcome of initial fluoride concentration was studied at their pH, optimum dose, and contact time on adsorbents onto various concentrations of fluoride solutions (10, 15, 20, 25, 30 mg/l). Fig. 5 describes the impact of initial fluoride concentration on the removal efficiency of fluoride. The results illustrated that fluoride removal potency ablated by increasing the initial fluoride concentration attributed to the fixed dose of adsorbent capacity adsorbents gets saturated at high concentration.

Pore volume and active sites of the adsorbents are stuffed by the fluoride, and its removal comes down. A similar trend has been reported for removal of fluoride using Neem charcoal [29].

The adsorption capacity of fluoride adsorbed per unit adsorbent (q_e) (mg/g) was calculated according to following equation [29].

$$q_e = \frac{(C_i - C_e)}{m} V \frac{mg}{g}$$

Where,

C_i: Initial fluoride concentration

C_e: Final fluoride concentration

V: Volume of the solution (l)

m: Mass of the adsorbent (g).

The result of Fig. 6 shows that the amount of adsorbed fluoride expands with the increase in fluoride initial concentrations. Turmeric has maximum adsorption among given two bio-adsorbent because of its lower adsorbent dose (mg) and high removal efficiency of MnO_2-coated turmeric (Table 1).

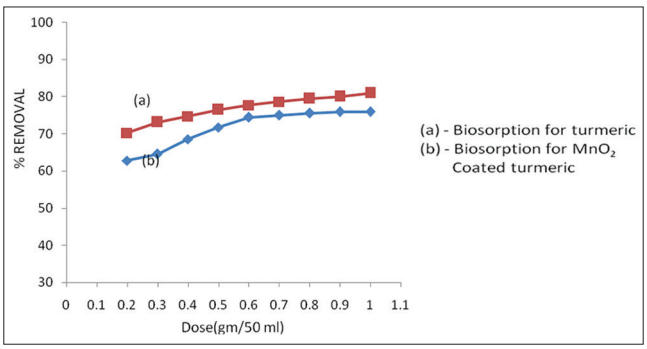

Fig. 3: Effect of dose on fluoride removal

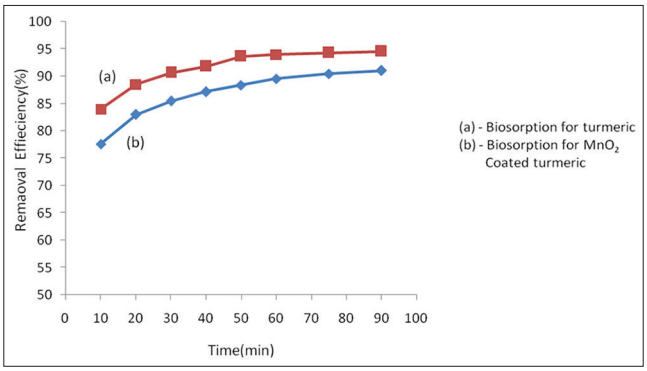

Fig. 4: Effect of contact time on fluoride removal efficiency

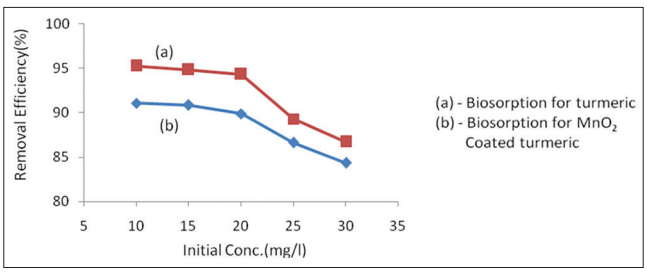

Fig. 5: The effect of initial fluoride concentration on removal efficiency

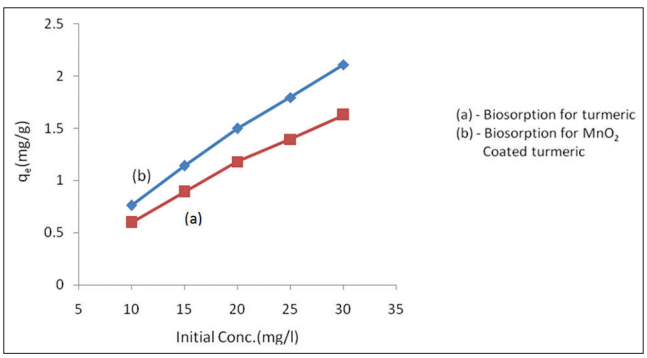

Fig. 6: The effect of initial fluoride concentration on fluoride desorption

Table 1: Data obtained such as pH, contact time, dose, concentration, adsorption capacity, and removal efficiency for both biosorbents

Adsorbents	pH	Contact time (minutes)	Dose (g/l)	Concentration (mg/l)	Adsorption capacity (mg/g)	Removal Efficiency (%)
Turmeric	7.0	75	12.0	20.0	1.498	89.90
MnO_2-coated turmeric	6.0	60	16.0	20.0	1.340	94.34

Table 2: Various kinetic parameters for pseudo-first order and pseudo-second order

Adsorbent	Pseudo-first order			Pseudo-second order		
	K_1	$q_{e\,(cal)}$	R^2	K_2	$q_{e\,(cal)}$	R^2
MnO_2-coated turmeric	0.039	0.202	0.974	0.434	1.369	0.999
Turmeric	0.053	0.0485	0.948	0.254	1.557	1

Adsorption kinetics

Adsorption kinetics explains mechanism of adsorption of fluoride on biosorbents. Adsorption kinetics models are intra-particle diffusion, pseudo-first order pseudo-first order as shown in Fig 7, and pseudo-second order. Studies of these models explain the adsorption behavior of fluoride on bio-adsorbents.

Pseudo-first order model

$$\log(q_e - q_t) = \log q_e - \frac{k_1}{2.303}t$$

Pseudo-second order model

$$\frac{t}{qt} = \frac{t}{qe} + \frac{1}{k2q_e^2}$$

Where,

q_e: Amount of fluoride adsorbed at equilibrium (mg/g)

q_t: Amount of fluoride adsorbed at time t (mg/g)

k_1: Kinetics rate constants for the pseudo-first order models (1/minutes)

k_2: Kinetics rate constants for the pseudo-second order models (g/mg min).

Using the Figure 8, we calculated the rate constant (k) of fluoride sorption for all adsorbents were calculated with the help of plotting the graph which are given below in Table 2.

From the Table 2, data show that the pseudo-second order is the best model for the adsorption for all adsorbent. Adsorption follows the pseudo-second order kinetic because of the better result for all adsorbents.

To determine adsorption study, rate-limiting step is necessary. Intra-particle diffusion as shown in Fig 9 and external mass transfer are two methods to explain the solid-liquid adsorption process for a solute. Intra-particle diffusion occurs in the case of the high speed of agitation (120 rpm) of solid-liquid test sample during the experiment. At very high agitation speed, it was reasonable to assume that mass transfer occurred from bulk of liquid to the particle adsorbents, the external surface was not limiting the rate. Yadav *et al*. report that both surface and intra-particle diffusion might be the rate-limiting step [30]. McKay in his research explained, the double nature of the diffusion, first linear portion of the plot depicts the boundary layer diffusion and second part of the linear portion depicts the intra-particle diffusion [31].

$$q_{(t)} = X_i + K_p * t^{0.5}$$

Where,

Table 3: Model parameters for intra-particle diffusion

Adsorbent	K_p	X_i	R^2
MnO_2-coated turmeric	0.026	1.132	0.921
Turmeric	0.033	1.221	0.929

q_t: Adsorption capacity (mg/g)

K_p: Diffusion constant (mg/g $min^{0.5}$)

X_i: Maximum capacity in case of intra-particle diffusion

From the plot, we have calculated the values of equation parameters (X_i, K_p) for all the adsorbents which are given in Table 3.

Equilibrium studies

All the models are explained in their linearized form. We have studied three models for the adsorption characteristics - Langmuir, Freundlich, and Temkin as shown in Figs. 10-15.

Langmuir model in linearized form

$$\frac{C_e}{q_e} = \frac{C_e}{q_m} + \frac{1}{bq_m}$$

Where,

C_e: Equilibrium concentration (mg/l)

q_m: Maximum adsorption capacity(mg/g)

b: Constant.

The magnitude of b reflects the slope of the adsorption isotherm which is a measure of adsorption affinity coefficient (1/mg).

Linearized Freundlich equation is given as:

$$\log\left(\frac{x}{m}\right) = \log K_f + \frac{1}{n}\log(C_e)$$

Where,

x: Amount of solute adsorbed (mg)

m : Mass of adsorbent used (g)

C_e: Equilibrium solute concentration in solution (mg/l)

K_f: Constant (1/g)

K_f is a measure of adsorption capacity and 1/n is a measure of adsorption intensity. The values of K_f and n were obtained from the slope and intercept of the plot between log (x/m) and log C_e. The Freundlich

Table 4: Depicts various Langmuir, Freundlich, and Temkin parameters observed and calculated during the experiments

Adsorbent	Langmuir			Freundlich			Temkin		
	b	q_m	R^2	K_F	n	R^2	A_T	b_T	R^2
MnO_2-coated turmeric	0.993	2.283	0.989	1.037	2.314	0.914	9.032	4860.86	0.967
Turmeric	0.359	3.344	0.979	0.893	1.709	0.959	3.060	3207.55	0.992

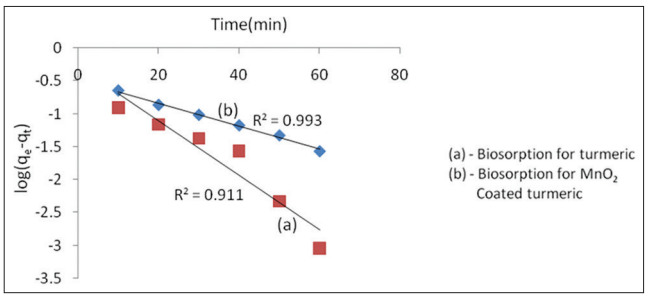

Fig. 7: Plot for pseudo-first order kinetics

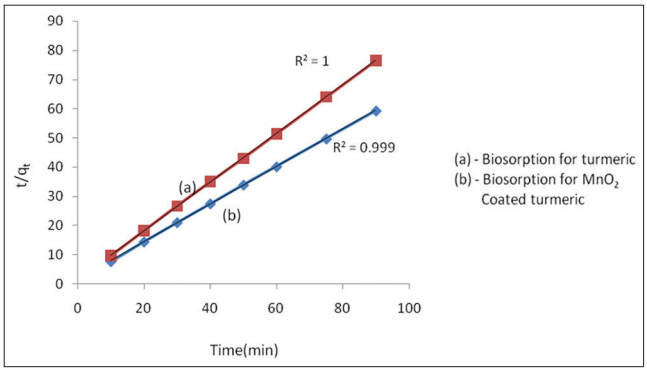

Fig. 8: Plot for pseudo-second order kinetics

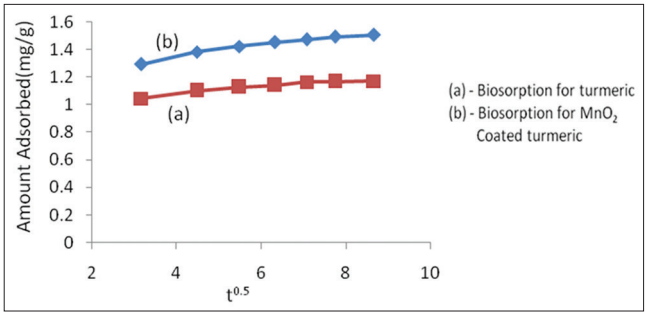

Fig. 9: Plots for intra-particle diffusion of fluoride in different adsorbents

equation deals with physio-chemical adsorption on heterogeneous surfaces.

Temkin model equation is given as:

$$q_e = \frac{RT}{b_T}\ln(A_T) + \frac{RT}{b_T}\ln(C_e)$$

Where,

R: Gas constant

T: Temperature (K)

C_e: Equilibrium concentration (mg/l)

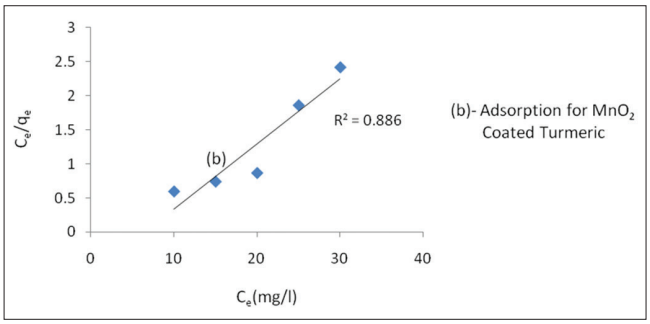

Fig. 10: Langmuir isotherm model for MnO_2-coated turmeric

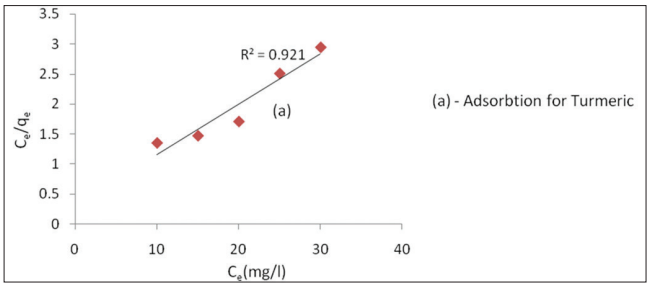

Fig. 11: Langmuir isotherm model for turmeric

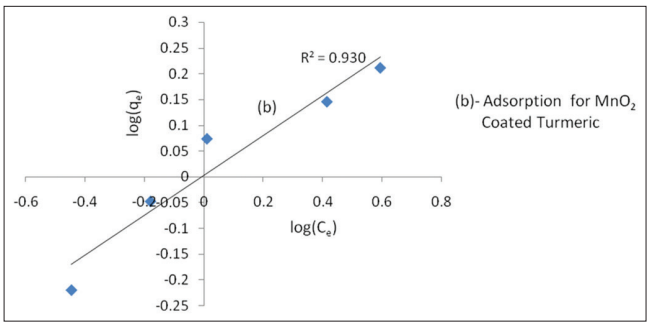

Fig. 12: Freundlich isotherm model for MnO_2-coated turmeric

A_T: Adsorption constants

b_T: Adsorption constants.

All the adsorption parameters have calculated from the linear plots of models which are given in Table 4.

By comparing the correlation coefficients R^2 values, we can verify the correlation coefficients are more than 0.97 for Langmuir, and other rest of the models have less value as compared to Langmuir isotherm model. Hence, the best fit model for all adsorbents is Langmuir adsorption model. It informs the adsorption experimental data was fitted well by the Langmuir isotherm.

Characterization of biosorbent

Fourier transform infrared spectroscopy (FTIR)

Functional groups present in biosorbents before and after adsorption of fluoride were determined using FTIR (Thermo Nicolet, Magna 7600).

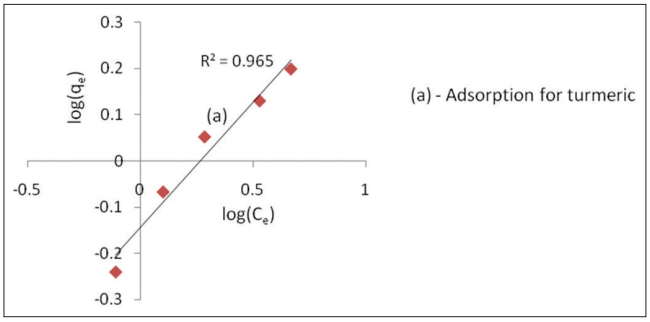

Fig. 13: Freundlich isotherm model for turmeric

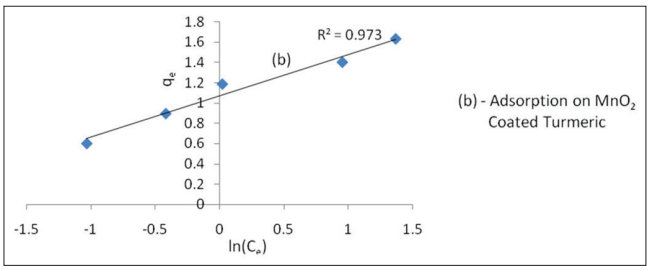

Fig. 14: Temkin isotherm model for MnO_2-coated turmeric

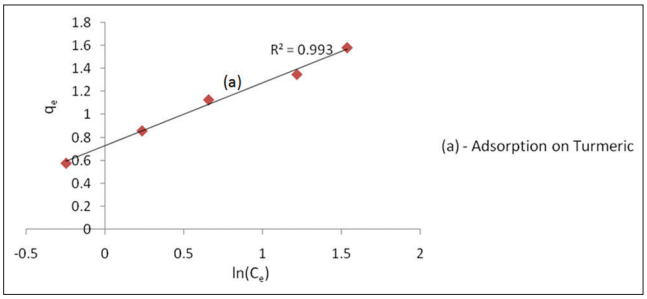

Fig. 15: Temkin isotherm model for turmeric

The samples were prepared by pellet (pressed disk) method by mixing the same amount of KBr in each sample. Fig. 16a and b, 17a and b show FTIR spectra of turmeric and MnO_2-coated turmeric within the spectral range of 4000-400 cm.

The range of different wave numbers assign the functional groups present in the adsorbent. The alcohol is seen in the range of 3200-3600 and 3500-3700 while alcohol with presence of phenol can be found out in the IR range of 970-1250. On a similar basis, alkenes are found in three IR ranges, namely, 1350-1480, 1620-1680, and 675-1000. Alkyl Halide with IR range of 500-600 is also seen with amines at 1550-1650. Carboxylic acids and derivatives were also observed at 2500-3300 as shown in Table 5.

Scanning electron micrograph (SEM) analysis

SEM for turmeric

SEM analysis has been used for investigating the surface morphology of the turmeric. Fig. 18a and b show the SEM of turmeric biosorbent used for adsorption studies. It was revealed from these figures that these adsorbents had irregular and porous surface. The difference in the adsorbent capacity of biosorbent was mainly due to the difference in their surface porosity.

SEM MnO_2-coated turmeric

The surface morphology of the MnO_2-coated turmeric was examined by SEM analysis. Fig. 19a and b show the SEM of MnO_2-coated turmeric used for adsorption studies. It was revealed from these figures that these adsorbents had irregular and porous surface. Moreover, the difference in the adsorbent capacity of biosorbent was mainly due to the difference in their surface porosity.

EDAX analysis

EDAX for turmeric

EDAX of turmeric before and after adsorption of fluoride ions was shown in Fig. 20a and b. From the analysis, it was clear that various elements, such as carbon, oxygen, and very small amount of potassium, were present in virgin adsorbent but fluoride was not present there. When the EDAX of the adsorbent was carried out after the adsorption

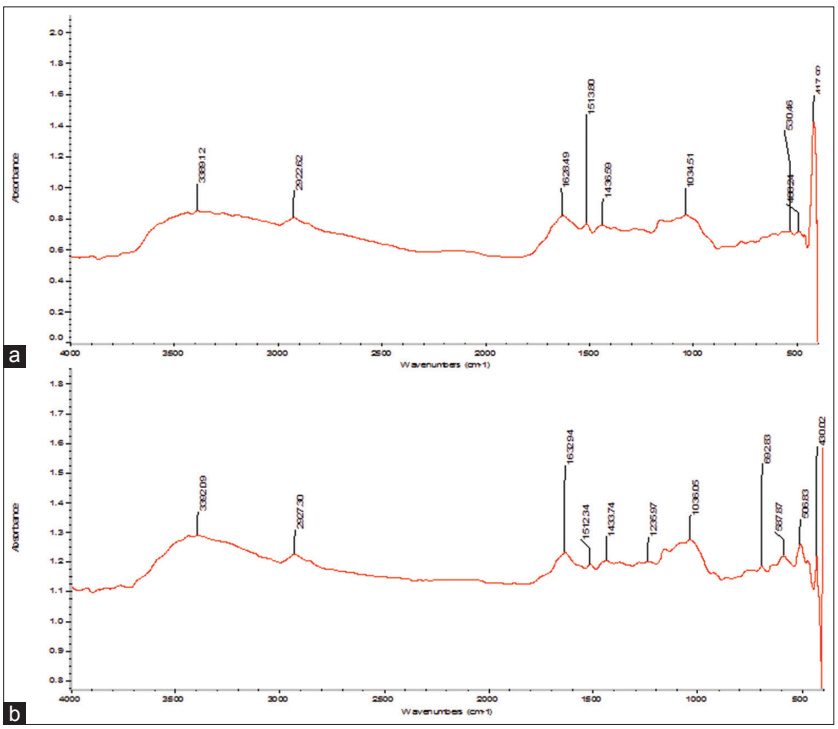

Fig. 16: (a) Pictorial representation of Fourier transform infrared spectroscopy (FTIR) of turmeric before experiment. (b) Pictorial representation of FTIR of turmeric after experiment

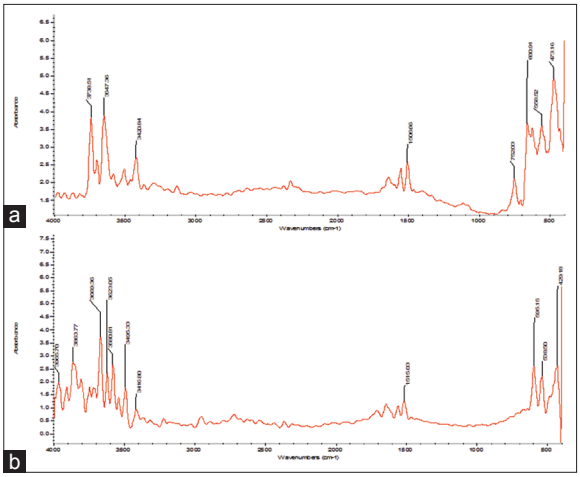

Fig. 17: (a) Pictorial representation of Fourier transform infrared spectroscopy (FTIR) of MnO_2-coated turmeric before experiment. (b) Pictorial representation of FTIR of MnO_2-coated turmeric after experiment

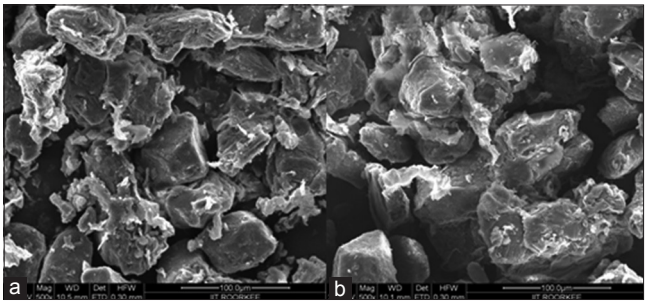

Fig. 18: Scanning electron micrograph image of turmeric (a) before adsorption (b) after adsorption

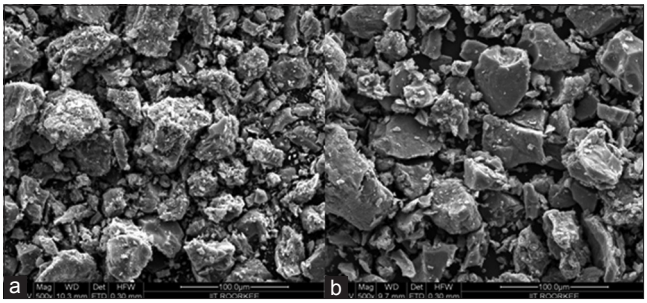

Fig. 19: Scanning electron micrograph image of MnO_2-coated turmeric (a) Before adsorption (b) After adsorption

of fluorides ion, fluoride was present on the surface of adsorbent about 9.26 wt % which confirmed the adsorption of fluoride by these adsorbents.

EDAX for MnO_2-coated turmeric

EDAX of MnO_2-coated turmeric before and after adsorption fluoride ions are shown in Fig. 21a and b. From these figures, it was clear that various elements such as oxygen and magnesium were present in virgin adsorbent, but fluoride was not present there. When the EDAX of the adsorbent was carried out after the adsorption of fluorides ion, fluoride was present on the surface of adsorbent about 7.49 wt % which confirmed the adsorption of fluoride by these adsorbents.

Comparing bio-adsorbents used in defluoridation process

Table 6 shows comparison of the defluoridation capacities of different biomass-based sorbents as shown in Table 6.

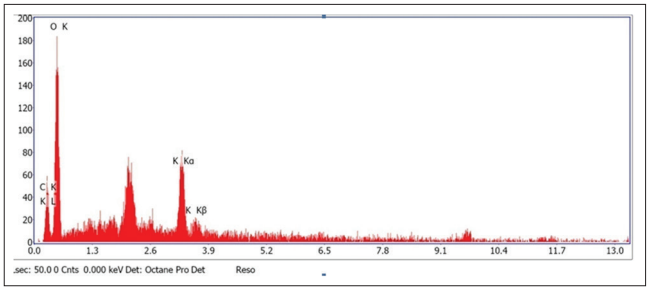

Element	Weight %	Atomic %	Net Int.	Error %
C K	20.26	26.86	7.25	14.27
O K	69.18	68.85	30.93	11.45
K K	10.56	4.3	16.33	11.41

Fig. 20a: EDAX image of turmeric before adsorption

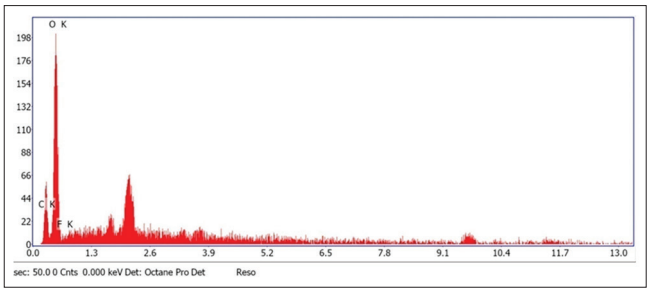

Element	Weight %	Atomic %	Net Int.	Error %
C K	25.73	32.01	7.82	14.24
O K	65.01	60.71	34.63	10.37
F K	9.26	7.28	2.13	29.54

Fig. 20b: EDAX image of turmeric after adsorption

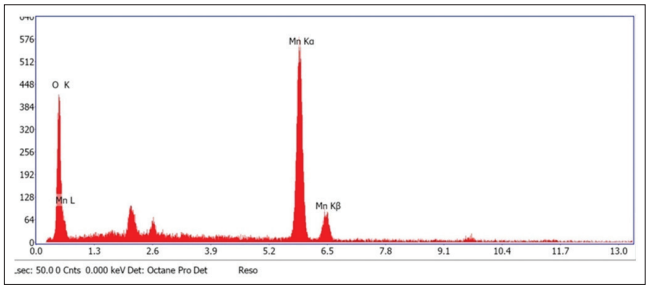

Element	Weight %	Atomic %	Net Int.	Error %
O K	22.34	49.69	69.56	7.24
MnK	77.66	50.31	168.06	2.83

Fig. 21a: EDAX image of MnO_2-coated turmeric before adsorption

CONCLUSIONS

Turmeric and MnO_2-coated turmeric biosorbents were studied for the removal of fluoride on synthetic waste water assuming as industrial waste water. The conclusion drained from the experiment is given below:

1. The MnO_2-coated turmeric and turmeric removed 94.34% and 89.9% of fluoride, respectively, from an aqueous solution of concentration 20 mg/l at pH of 6.0 and 7.0, respectively
2. Contact time for MnO_2-coated turmeric and turmeric are 60.0 and 75.0 minutes and dose 14 and 12 g/l, respectively
3. Mechanism of adsorption kinetics was found to be pseudo-second order reaction, and the mechanism of fluoride removal on adsorbents was found to be complex. The surface adsorption as well as intra-

Table 5: FTIR analysis for adsorbent in tabular form

Wave number (cm^{-1})	Compound	Groups
3200-3600	Alcohol	O-H
2500-3300	Carboxylic acids and derivatives	O-H (very broad)
1550-1650	Amines	NH_2 scissoring (1° amines)
1350-1480	Alkane	-C-H
970-1250	Alcohols and phenols	C-O
500-600	Alkyl halide	C-Br
1620-1680	Alkene	C=C
675-1000	Alkene	=C-H
3500-3700	Alcohol	O-H

FTIR: Fourier transform infrared spectroscopy

Table 6: Comparison of the defluoridation capacities of different biomass-based sorbents

Adsorbent	pH	Adsorption capacity (mg/g)	References
Powdered biomass *Tinospora cordifolia*	7.0	25	Pandey *et al.* (2012)
Ca-treated *Anabaena fertilissima*	-	7.0	Bhatnagar *et al.* (1991)
Ca-treated *Chlorococcum humicola*	-	4.5	Bhatnagar *et al.* (1991)
Biomass carbon prepared at 300°C	5.8	0.52	Sinha *et al.* (2003)
Biomass carbon prepared at 600°C	-	1.54	Sinha *et al.* (2003)
Spirodela polyrrhiza	-	0.91	Shirke and Chandra (1991)
Used tea leaves	1.5	0.51	Methodis and Selvapathy (2005)
Moringa indica-based activated carbon	2.0	0.23	Karthikeyan and Llango (2007)
Powdered biomass (*Azadirachta indica+Ficus religiosa+ Acacia catechu wild)*	2.0	0.04	Jamode *et al.*, 2004a and Jamode *et al.*, 2004b
Spirogyra sp.-IO1	2.0	1.27	Mohan *et al.* (2007a)
Spirogyra sp.-IO2	7.0	1.27	Mohan *et al.* (2007b)
Activated carbon derived from rice straw	2.0	15.90	Daifullah *et al.* (2007)
Pine wood biochar	2.0	7.66	Mohan *et al.* (2012)
Pine wood biochar	2.0	9.77	Mohan *et al.* (2012)
Ammonium carbonate activated carbon of *Turmericus indica* fruit shells	7.05	22.33	Sivasankar *et al.* (2012)
Zirconium (iv)-impregnated ATFS (*Arachis hypogia*) shell carbon	-	2.32	Alagumuthu and Rajan (2010a)
Cynodon dactylon-based activated carbon	7.0	4.617	Alagumuthu *et al.* (2011)
Zirconium impregnated cashew nut (*Anacardium occidentale*) shell carbon	7.0	1.83	Alagumuthu and Rajan (2010b)
Phyllanthus emblica-based thermally activated carbon	7.0	7.014	Veeraputhiran and Alagumuthu (2011)
Pecan (*Carya illinoinensis*) nut shells carbon modified with egg shells calcium	7.0	1.61–2.51	Hernández-Montoya *et al.* (2012)
Scandinavia spruce wood modified with aluminum and iron oxides and carbonized at 500°C	6.9	7.92	Tchomgui-Kamga *et al.* (2010)
Scandinavia spruce wood modified with aluminum and iron oxides and carbonized at 650°C	6.9	13.64	Tchomgui-Kamga *et al.* (2010)
Scandinavia spruce wood modified with aluminum and iron oxides and carbonized at 900°C	6.9	5.67	Tchomgui-Kamga *et al.* (2010)
Sawdust raw	6.0	1.73	A. K. Yadav *et al.*
Wheat straw raw	6.0	1.93	A. K. Yadav *et al.*
Activated bagasse carbon	6.0	1.15	A. K. Yadav *et al.*
Turmeric	7.0	1.1793	Current study [1]
MnO_2 treated turmeric	6.0	1.498	Current study [1]

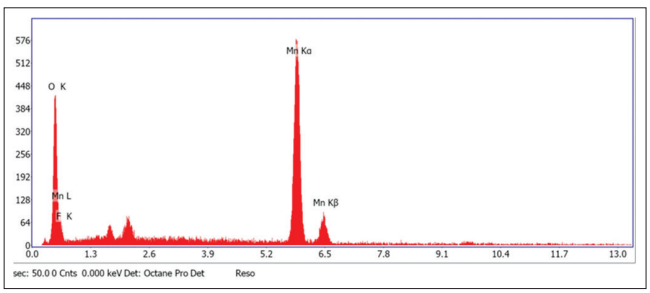

Element	Weight %	Atomic %	Net Int.	Error %
O K	20.36	42.7	72.29	6.83
F K	7.49	13.23	4.75	22.12
MnK	72.16	44.07	174.96	2.68

Fig. 21b: EDAX image of MnO2-coated turmeric after adsorption

particle diffusion contributes to the rate-determining step

4. High removal efficiency of adsorbent MnO_2-coated turmeric and turmeric is detected
5. Presence of others ions in groundwater did not significantly affect the defluoridation process
6. Adsorption isotherm models Langmuir, Freundlich, and Temkin were studied. Out of these, the best plots for adsorption isotherm were Langmuir model.

REFERENCES

1. Maharamanlioglu M, Kizilcikli I, Bicer IO. Adsorption of fluoride from aqueous solution by acid treated spent bleaching earth. J Fluorine Chem 2002;115:41-7.
2. Sorg TJ. Treatment technology to meet the interim primary drinking water regulations for inorganics. Am Water Works Assoc J 1978;70(12):105-11.
3. Treshow M, Anderson FK. Plant Stress from Air Pollution. New York: Wiley; 1989. p. 44.

4. Pushnik JC, Miller GW. The influences of elevated environmental fluoride on the physiology and metabolism of higher-plants. Fluoride 1990;23(1):5-19.
5. Susheela AK. Prevention and Control of Fluorosis in India. Health Aspect. Vol. 1. New Delhi, India: Rajiv Gandhi National Drinking Water, Mission; 1993.
6. Bhatnagar M, Bhatnagar A. Algal and cyanobacterial responses to fluoride. Fluoride 2000;33(2):55-65.
7. Mangla B. India dentists squeeze fluoride warnings off tubes. New Scientist 1991;131:16.
8. Chinoy NJ. Effects of fluoride on physiology of animals and human beings. Indian J Environ Toxicol 1991;1(1):17-32.
9. Raichur AM, Basu MJ. Adsorption of fluoride onto mixed rare earth oxides. Sep Purif Technol 2001;24(1-2):121-7.
10. Lv L, He J, Wei M, Evans DG, Duan X. Factors influencing the removal of fluoride from aqueous solution by calcined Mg–Al–CO 3 layered double hydroxides. J Hazard Mater 2006;133(1-3):119-28.
11. Saha S. Treatment of aqueous effluent for fluoride removal. Water Res 1993;27:1347-50.
12. Reardon EJ, Wang Y. A limestone reactor for fluoride removal from waste waters. Environ Sci Technol 2000;34(15):3247-53.
13. Singh G, Kumar B, Sen PK, Majumdar J. Removal of fluoride from spent pot liner leachate using ion exchange. Water Environ Res 1996;71:36-42.
14. Wang R, Li H, Wang Y. Study of a new adsorbent for fluoride removal from water, water quality. Res J Can 1995;30(1):81-8.
15. Lai YD, Liu JC. Fluoride removal from water using spent catalyst. Sep Sci Technol 1996;31:2791-7.
16. Chaturvedi AK, Yadav KP, Pathak KC, Singh VN. Defluoridation of water by adsorption on fly ash. Water Air Soil Pollut 1990;49(1):51-61.
17. Mayadevi S. Adsorbents for the removal of fluoride from water. Ind Chem Eng 1996;A38:155-7.
18. Bhargava DS, Killedar DJ. Fluoride adsorption on fishbone charcoal through a moving media adsorber. Water Res 1992;26(6):781-8.
19. Hichour M, Persin F, Sandeaux J, Gavach C. Fluoride removal from water by Donnan analysis. Sep Purif Technol 2000;18(1):1-11.
20. Meenakshi, Maheswari RC. Fluoride in drinking water and its removal. J Hazard Mater 2006;137(1):456-63.
21. Prakasam RS, Chandrareddy PL, Manisha A, Ramakrishna SV. Defluoridation of drinking water using *Eichhornia* sp. IJEP 1998;19(2):119-24.
22. Mohan SV, Bhaskar YV, Karthikeyan J. Biological decolourization of simulated azo dye in aqueous phase by algae *Spirogyra* species. Int J Environ Pollut 2003;21(3):211-22.
23. Mohan SV, Karthikeyan J. Removal of lignin and tannin aqueous solution by adsorption onto activated charcoal. Environ Pollut 1997;97(1-25):183-97.
24. Ilhami T, Bayramoğlu G, Yalçin E, Başaran G, Celik G, Arica MY. Equilibrium and kinetic studies on biosorption of Hg(II), Cd(II) and Pb(II) ions onto micro algae *Chlamydomonas reinhardtii*. J Environ Manage 2005;77(2):85-92.
25. Killedar DJ, Bhargava DS. Effects of stirring rate and temperature on fluoride removal by fishbone charcoal. Indian J Environ Health 1993;35(2):81-7.
26. Onyango MS, Kojima Y, Aoyi O, Bernardo EC, Matsuda M. Adsorption equilibrium modelling and solution chemistry dependence of fluoride removal from water by trivalent-cation-exchanged zeolite. J Colloid Interface Sci 2006;279(2):341-50.
27. Onyango MS, Kojima Y, Kuchar D, Kubota M, Matsuda H. Uptake of fluoride by Al^{3+} - Pretreated low-silica synthetic zeolites: Adsorption equilibria and rate studies. Sep Sci Technol 2001;41(4):1-22.
28. Ramanaiah SV, Mohan SV, Sarma PN. Adsorptive removal of fluoride from aqueous phase using waste fungus (*Pleurotus ostreatus* 1804) biosorbent: Kinetics evaluation. Ecol Eng 2007;31(1):47-56.
29. Chakrabarty S, Sharma HP. Defluoridation of contaminated drinking water using neem charcoal adsorbent: Kinetics and equilibrium studies. Int J ChemTech Res 2012;4(2):511-6.
30. Fan X, Parker DJ, Smith MD. Adsorption kinetics of fluoride on low cost materials. Water Res 2003;37(20):4929-37.
31. McKay G, Otterburn MS, Sweeny AG. The removal of colour from effluent using various adsorbents III. Silica: Rate processes. Water Res 1980;14:15-20.